engineering proceedings

MDPI

Proceeding Paper

Design Considerations of a Vibration Absorber with Nonlinear Stiffness for Power Electric Units †

Zoltan Gabor Gazdagh [1,*], Zoltan Gabos [2,3], Ádám Szabó [4], Bálint Dobrovics [4], Szargisz Szargszjan [4], Szabolcs Nagy [4,5] and Zoltan Dombovari [2,3]

[1] Engineering Acoustics—Noise Vibration and Harshness, Robert Bosch Kft., Gyömrői út 104, H-1103 Budapest, Hungary
[2] Department of Applied Mechanics, Faculty of Mechanical Engineering, Budapest University of Technology and Economics, Műegyetem rkp. 3, H-1111 Budapest, Hungary; zoltan.gabos@mm.bme.hu (Z.G.); dombovari@mm.bme.hu (Z.D.)
[3] MTA-BME Lendület Machine Tool Vibration Research Group, Department of Applied Mechanics, Budapest University of Technology and Economics, H-1111 Budapest, Hungary
[4] Electrified Motion—Inverter, Robert Bosch Kft., Gyömrői út 104, H-1103 Budapest, Hungary; adam.szabo5@hu.bosch.com (Á.S.); balint.dobrovics@hu.bosch.com (B.D.); szargisz.szargszjan@hu.bosch.com (S.S.); szabolcs.nagy@hu.bosch.com (S.N.)
[5] Electrified Motion—Inverter Mechanics, Simulation, Robert Bosch Kft., Gyömrői út 104, H-1103 Budapest, Hungary
* Correspondence: zoltangabor.gazdagh@hu.bosch.com
† Presented at the Sustainable Mobility and Transportation Symposium 2025, Győr, Hungary, 16–18 October 2025.

Abstract

Power electronic units (PEUs) in electric drivetrains are subjected to vibration loads that may lead to component fatigue through resonance. This research aims to understand the behavior of passive vibration absorbers and to establish a design approach for them. The proposed systematic design of a nonlinear tuned mass damper (NTMD) for PEUs begins with the separate linear experimental analyses of the PEU and passive absorber. This linear approach is possible due to the Hartman–Grobman theorem. Then the nonlinearity is quantified through frequency sweep measurements. A two-degree-of-freedom (DoF) coupled model is developed for the NTMD, which can be used for analyzing certain parameter changes. To manage the load-dependent responses inherent to nonlinear behavior, design constraints on the attenuated bandwidth and absorber stiffness are introduced, providing clear and optimizable targets. By extending classical linear absorber design principles to nonlinear regimes, the proposed method enhances the durability and reliability of PEU components.

Keywords: vibration absorber; nonlinearity; tuned mass damper

check for updates

Academic Editors: Szabolcs Kocsis-Szürke, Dániel Csikor and Boglárka Eisinger Balassa

Published: 29 October 2025

Citation: Gazdagh, Z.G.; Gabos, Z.; Szabó, Á.; Dobrovics, B.; Szargszjan, S.; Nagy, S.; Dombovari, Z. Design Considerations of a Vibration Absorber with Nonlinear Stiffness for Power Electric Units. *Eng. Proc.* **2025**, *113*, 20. https://doi.org/10.3390/engproc2025113020

Copyright: © 2025 by the authors. Licensee MDPI, Basel, Switzerland. This article is an open access article distributed under the terms and conditions of the Creative Commons Attribution (CC BY) license (https://creativecommons.org/licenses/by/4.0/).

1. Introduction

In the field of hybrid and electric vehicles, the power electronic unit (PEU), commonly referred to as the inverter, serves as a critical component that plays an essential role in the overall functionality and performance of the vehicle [1]. Its primary function is to convert the direct current (DC) supplied by the battery into alternating current (AC) that powers the electric machine. The reliability and efficiency of the PEU are crucial, as they directly influence the vehicle's overall performance, energy efficiency, and user experience. Given that PEUs are typically mounted directly onto or in close proximity to the electric engine, vibration, alongside thermomechanical effects become a significant

concern that must be addressed [2]. Excessive vibrations can lead to premature wear and fatigue of components, ultimately reducing the lifespan of a PEU and affecting the vehicle's operational reliability. Therefore, it is crucial that during the design phase of the PEU, greater emphasis is placed on developing designs that are robust against vibration. This can be achieved by strategically shifting resonance frequencies away from critical regions or by incorporating effective damping elements to reduce amplitude [3]. Passive vibration absorbers, including tuned mass dampers (TMDs) and viscous dampers, provide effective, maintenance-free solutions that can significantly reduce resonant responses in various applications [3]. These absorbers offer advantages over traditional solutions by minimizing the need for active control systems and reducing maintenance requirements.

This study aims to briefly cover the fundamental principles of designing TMDs [3,4], by proposing a systematic step-by-step design procedure, and highlight the crucial role of mass ratio in determining the overall performance of the system. The attached absorber shows significant nonlinear behavior in this study. Therefore, our systematic proposition considers a nonlinear tuned mass damper (NTMD) [5], where load-dependent response curves are extracted for the coupled system, consisting of the PEU and the nonlinear absorber. To tune the NTMD, our proposition suggests the extraction of locally (small amplitude vibrations) linear parameters first [6]. Then, the experimental identification of the nonlinear parameter is carried out [7]. Finally, the absorber is designed through numerical simulations on the identified mechanical structure. Here, we constrain the frequency range and the stiffness of the absorber to obtain a clear and optimizable set of parameters.

The remainder of this study consists of the brief introduction of linear TMD design considerations. Then, the systematic nonlinear identification of the absorber and the tuning of the NTMD is discussed in detail. We show this procedure through the mass tuning of a given absorber within a predefined frequency range. Finally, a summary of our findings is shown to the reader.

2. Design Considerations of Linear Vibration Absorbers

Vibration absorbers play a critical role in engineering systems by reducing undesirable vibrations, protecting equipment, enhancing performance, and improving comfort and safety. The precise design of TMDs [3] ensures efficient vibration mitigation in mechanical structures, with the primary goal to minimize the response amplitude of the primary structure, m_1 in Figure 1. Achieving this goal involves optimizing several parameters, such as the damping coefficient, mass ratio, stiffness, natural frequencies and the mounting location. This section will briefly discuss these factors and present guidelines for effectively sizing linear TMDs.

The mass ratio μ is defined as the relation between the added absorber mass m_2 and the original mass m_1, visualized in Figure 1c. Typically, a higher mass ratio improves the bandwidth of the vibration attenuation on the primary structure m_1. However, excessively high mass ratios can negatively affect the overall system by introducing an unfeasible mass, increasing costs, and neglecting practicality. Optimal mass ratios usually range between 0.05 and 0.2 in practice, balancing efficiency and feasibility. This study builds on the mechanical model, introduced in Figure 1c. The mathematical formulation of this model can be written as

$$m_1\ddot{x}_1 + c_1\dot{x}_1 + c_2(\dot{x}_1 - \dot{x}_2) + k_1x_1 + k_2(x_1 - x_2) = F_1(t), m_2\ddot{x}_2 + c_2(\dot{x}_2 - \dot{x}_1) + k_2(x_2 - x_1) = 0, \quad (1)$$

where m_1, k_1, and c_1 are the apparent mass, stiffness and damping coefficient of the attenuated structure, respectively. The external force in the structure is defined as $F_1(t) := F_{1,1} \cos \omega_F t$ Similarly, m_2, k_2, and c_2 are the parameters regarding the standalone

absorber mass (Figure 1a,b). The displacements of the two masses are denoted by x_1 and x_2, respectively. Finally, the forcing amplitude, acting on m_1, is F_1, with ω forcing angular frequency. The system parameters are extracted through conventional modal testing techniques and summarized in Table 1.

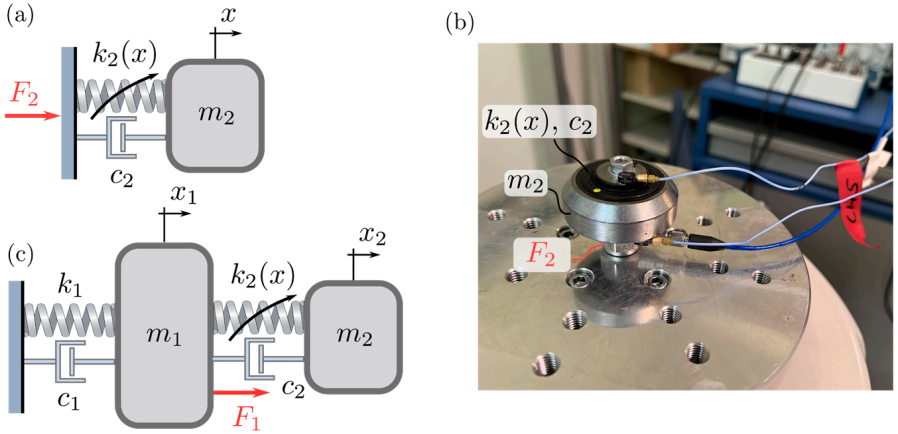


Figure 1. Mechanical model of the absorber (**a**) and its physical setup (**b**) to measure its frequency response curves. Panel (**c**) shows the coupled model, where the vibration absorber is attached to a structure m_1. Note that $k_2(x) = k_2 x + \beta x^3$ and $F_1(t) = F_{1,1} \cos \omega\, t$.

Table 1. Original system parameters from the experimental modal analysis of the TMD for the linear regime. After tuning the antiresonance to be at the resonance of the original structure $m_2 = 0.364$ kg.

	m_i (kg)	k_i (N/m)	c_i (Ns/m)	Driving Force:
$i = 1$	5.979	$24{\cdot}10^6$	646.9	$\omega \in [200,\ 400]$ Hz
$i = 2$	0.2	$1.46{\cdot}10^6$	21.6	$F_{1,1} \in [1,\ 200]$ N

Then, the formulation of the mass ratio μ and the dimensionless squared normalized frequency Ω are written as

$$\mu := \frac{m_2}{m_1},\ \Omega := \frac{\omega_n^2}{\omega_1^2}\,, \tag{2}$$

where ω_1 is the natural frequency of the standalone structure ($\omega_1^2 = k_1/m_1$), while m_1, and ω_n is the natural frequency of the coupled structure. For showing the basic principle of primary system response minimalization, let c_1 and c_2 be zero. In such a case, the response displacement of the primary mass m_1 is

$$H_{11}(\omega) := \frac{F_1(\omega)}{x_1(\omega)} = \frac{-\omega^2 m_2 + k_2}{\left(-\omega^2 m_1 + k_1 + k_2\right)\left(-\omega^2 m_2 + k_2\right) - k_2^2}, \tag{3}$$

where H_{11} (forcing and response are both at m_1) denotes the frequency response function (FRF) of (1) without any damping. The response amplitude of m_1 is minimized when the absorber parameters m_2 and k_2 are tuned close to the primary system's natural frequency [3]. Mathematically, optimal tuning occurs when

$$\left(-\omega^2 m_2 + k_2\right) = 0. \tag{4}$$

This means that the TMD must be tuned to the resonant frequency of the standalone structure:

$$\frac{k_2}{m_2} = \frac{k_1}{m_1}. \tag{5}$$

Introducing the absorber will create a coupled system, where the first resonance of the new system is $\omega_{n,1}$ and the second is $\omega_{n,2}$ (with the target ratio: $\Omega := \omega_{n,1,2}^2/\omega_1^2$) in such order that $\omega_{n,1} < \omega_1 < \omega_{n,2}$; see Figures 2 and 3. Combining (1) and (2) after simplification and setting $F_{1,1} = 0$ in (1), leads to the following characteristic equation:

$$\Omega^2 - (2+\mu)\Omega + 1 = 0. \tag{6}$$

Using the quadratic formula and exploiting $\Omega\omega_1^2 = \omega_n^2$ lead to the following:

$$\omega_{n,1,2}^2 = \omega_1^2\left(1 + \frac{\mu}{2} \pm \sqrt{\mu + \frac{\mu^2}{4}}\right). \tag{7}$$

This means that the two coupled natural frequencies $\omega_{n,1}$ and $\omega_{n,2}$ are split approximately symmetrically around the standalone ω_1 when $\mu << 1$. Then each offset is approximately $1/2\sqrt{\mu}\ \omega_1$. However, for larger mass ratios, the offset becomes asymmetric as Figure 2 shows. Note that the greater mass ratio will make wider frequency splits, suggesting a more effective absorber design as in Figure 2.

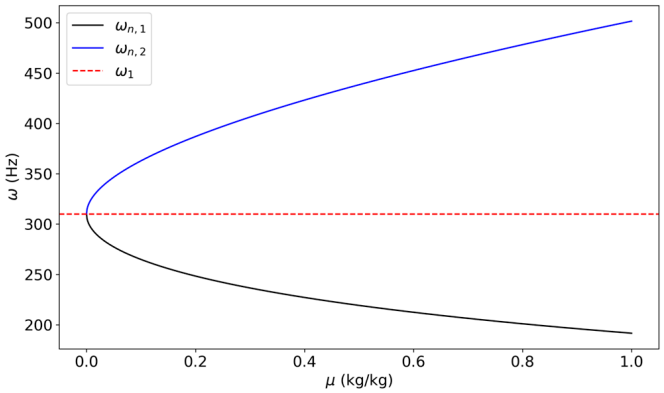


Figure 2. Demonstration of the coupled system's natural frequencies ($\omega_{n,1}$, $\omega_{n,2}$) compared to the standalone ω_1 as the mass ratio μ changes. The symmetry only holds for small μ values.

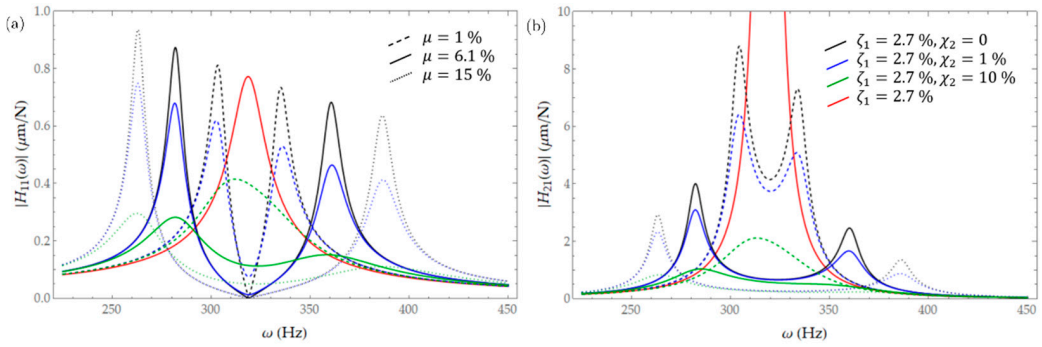


Figure 3. Frequency response functions (FRFs), based on the linear assumption, showing the effect of different mass ratios μ and TMD damping factor χ_2 in Den Hartog sense, where $\zeta_1 = 2.7\%$, while the critical TMD damping ratios are $\chi_{2,cr} = (6.2,\ 13.0,\ 15.4)\%$ according to (8) for the depicted $\mu = (1,\ 6.1,\ 10.0)\%$ cases (dashed, continuous, dotted): (**a**) FRFs of the primary mass and excitation is on the primary mass $H_{11}(\omega)$, red dashed line shows the target frequency ω_1= 319 Hz; (**b**) FRFs of the tuning mass and excitation is on the primary mass $H_{21}(\omega)$.

The damping coefficient c_1 determines the rate of the vibrational energy dissipation from the standalone structure, which usually results in a low standalone damping ratio (ζ_1 = 0.1% to 20%), causing the actual problematic peak in the first place (see red curves in Figure 3 with $\zeta_1 = 2.7\%$).

The TMD's damping c_2 is a design parameter, which is historically defined to the standalone natural frequency of the structure as $\chi_2 := c_2/(2m_2\omega_1)$ [3]. Increasing χ_2, the validity of (4) gradually decreases. In fact, ideally, we prefer this value to be vanished as (3) suggests; however uncertainties in the structural properties require increased bandwidth in so-called antiresonance attenuation. This can be achieved with moderate added damping through χ_2. One can assume any damping is welcomed; however it must be kept at least under, e.g., one of the lowest invariant points in the Den Hartog sense [3] to actually have antiresonance, resulting in

$$\chi_2^2 < \chi_{2,\mathrm{cr}}^2 := \frac{\mu(2+\mu)}{4\,(1+\mu)\left(1+\mu+2\,\sqrt{\mu(2+\mu)}\right)}. \tag{8}$$

With the presented data in Table 1, this limiting Den Hartog's damping factor is $\chi_2 < \chi_{2,\mathrm{cr}} = 13$ % with mass ratio $\mu = 6.1$ % which is determined with the tuned mass $m_2 = 0.364$ kg according to (5). In Figure 3, different FRFs are depicted related to the direct (driving) ones in the structure $\mathrm{H}_{11}(\omega)$ (Figure 3a) and the cross-FRF $\mathrm{H}_{21}(\omega)$ (Figure 3b) between the structure and the TMD showing its relative motion to the structure. The different mass ratios are shown with different line styles ($\mu = (1,\ 6.1,\ 15.0)$%, (dashed, continuous, dotted)), while different TMD damping ratios in Den Hartog sense are shown with black, blue and green colors in an order of $\chi_2 = (0,\ 1,\ 10)$%.

One can realize all of the presented cases have antiresonance except the one with the lowest mass ratio with the highest damping for the TMD χ_2, when $\mu = 1$% and $\chi_2 = 10$% for which the critical damping was $\chi_{2,\mathrm{cr}} = 6.2$ % according to (8).

3. Design Considerations of Nonlinear Vibration Absorbers

Although designing linear TMDs is a common and well-developed field in engineering [3,4], the materials used (especially rubber) can lead to nonlinear behavior for high forcing amplitudes [7]. Then, the effective design of a nonlinear tuned mass damper (NTMD) [5] becomes more challenging as the resonance depends on the forcing amplitude [8]. For this particular example, in this study, we assume the following equations of motion, based on the model in Figure 1:

$$m_1\ddot{x}_1 + c_1\dot{x}_1 + c_2(\dot{x}_1 - \dot{x}_2) + k_1x_1 + k_2(x_1 - x_2) + \beta(x_1 - x_2)^3 = F_{1,1}\cos\omega t, m_2\ddot{x}_2 + c_2(\dot{x}_2 - \dot{x}_1) + k_2(x_2 - x_1) + \beta(x_2 - x_1)^3 = 0, \tag{9}$$

where the only difference from (1) is the non-zero nonlinear parameter β. This way, the system is coupled through the combined linear k_2 and nonlinear β springs.

Finding an optimal or efficient parameter set for the nonlinear vibration absorber is not a straightforward task as was in Section 2 or in [3,4]. First, we have to characterize the nonlinearity of the single DoF absorber

$$m_2\ddot{x} + c_2\dot{x} + k_2x + \beta x^3 = F_2\cos\omega\, t, \tag{10}$$

which is already challenging in most cases [7,9]. Two key features are usually extracted to describe vibrating nonlinear structures. First, the so-called backbone curve (BBC) [8] (see Figure 4) which describes the vibration amplitude as a function of the vibration frequency during a free decay [8]. Secondly, the nonlinear frequency response curves (NLFR) (Figure 4) can be used for visualizing the shifting of the resonance frequency as the forcing amplitude grows [8]. Extracting these two features helps the parameter fitting of the mechanical system (8).

In this study, we use slow bi-directional frequency sweeps to extract the NLFR curves of the standalone vibration absorber (Figure 4). Note that these curves are only comparable with ideal nonlinear models like the one in (10) if the input force amplitude that excites the

structure is constant [8]. Therefore, either a force controller must be used, or the measured curves must be resectioned [8] at constant forcing amplitudes. Then, the NLFR curves can be presented (as in Figure 4) for the nonlinear vibration absorber in Figure 1b). By picking the maximum amplitudes of the NLFR curves, we get a good approximation (green crosses in Figure 4) of the BBC if the damping is relatively low in the structure [10].

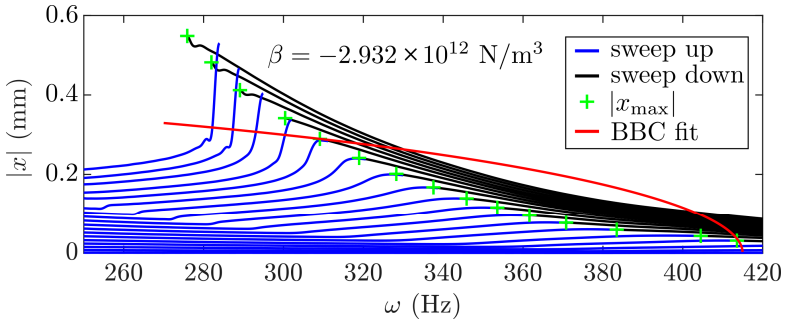


Figure 4. Up and down frequency sweeps on the standalone nonlinear vibration absorber. The maximum response amplitudes mark the BBC of the system, for which a cubic BBC was fitted to analyze the simplest behavior of NTMDs.

A cubic BBC can be fitted for the extracted data point by the following equation:

$$A(\omega) = 2\sqrt{\frac{\omega^2 - \omega_1^2}{3\gamma}}, \tag{11}$$

derived from the Poincaré–Linstedt solution of an undamped Duffing oscillator [9]. Note that $\gamma := \beta/m$ is the normalized nonlinear parameter, and $A(\omega)$ is the BBC of the standalone vibration absorber with the local (linear) natural frequency ω_2. The fitted curve for the extracted data is visualized in Figure 4. Although we acknowledge that the best fit for this case is not the cubic nonlinear oscillator, the simplicity of it enables us to qualitatively analyze the simplest case of a NTMD, which somewhat resembles the observed nonlinear absorber.

Having a grasp on the simplified mechanical model of the problem enables us to execute numerical simulations of the frequency sweeps that are related to the coupled structure, modeled by (9). To achieve an effective operation of the NTMD, one has to define goals to constrain the search for good passive absorber parameters (m_2 and k_2). For this particular case, we have set the following constraints:

- Attenuated frequency bandwidth: $\omega \in [200,\ 300]$ Hz.
- Feasible absorber mass range: $m_2 \in [0.124,\ 0.5]$ kg.
- Forcing amplitude range: $F_{1,1} \in [1,\ 300]$ N.
- Goal: minimizing the response amplitude of m_1 within the suggested frequency bandwidth.

With a clear set of goals in mind, the numerical tests can be methodically executed to find the most effective solution for the problem at hand. We propose carrying out numerical frequency down-sweep tests, since this case is a softening nonlinearity, with $F_{1,1} = 1$ N and m_2 incremented from 0.124 kg until 0.5 kg between the frequency sweeps. From this set of numerical tests, store the maximum response amplitude of x_1 for every sweep. This procedure has to be repeated $M \in \mathbb{N}^+$ times, while we store the maximum values in a set $x_{1,\max} \in \mathbb{R}^{N \times M}$, where N is the number of simulated sweeps and M is the number of forcing amplitudes. Figure 5 shows the visual representation of $x_{1,\max}$ for both the linear (grey) and nonlinear (red) cases. By finding the minimum in $x_{1,\max}$ at every forcing amplitude, one can obtain the most feasible m_2 parameter for the different loads considered in this case. It can be observed that increasing the parameter m_2 significantly improves the

attenuation capabilities of the absorber, meaning that for both the TMD and NTMD, the most effective absorber mass is $m_2 = 0.364$ kg with the set goals in mind.

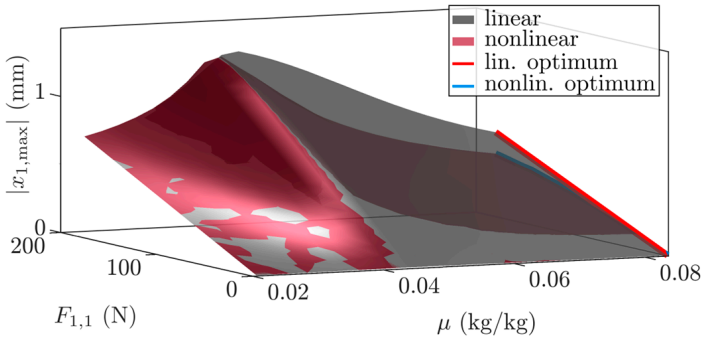


Figure 5. The grey (linear) and red (nonlinear) surfaces visualize the maximum response amplitudes of a given $F_{1,1}$ and μ parameter set within the bandwidth of interest. The two marked lines show that for both nonlinear and linear cases the most efficient mass ratio is at 0.08 kg/kg for all forcing amplitudes $F_{1,1}$.

Finally, let us demonstrate the difference between the TMD and NTMD with the chosen m_2 parameter. As shown in Figure 6, both absorbers are attenuating the response amplitudes within the frequency bandwidth of interest, with the addition of bistable regions in the nonlinear case. We also present the numerical continuation (executed in COCO [11]) of the NTMD for the observed case in Figure 7.

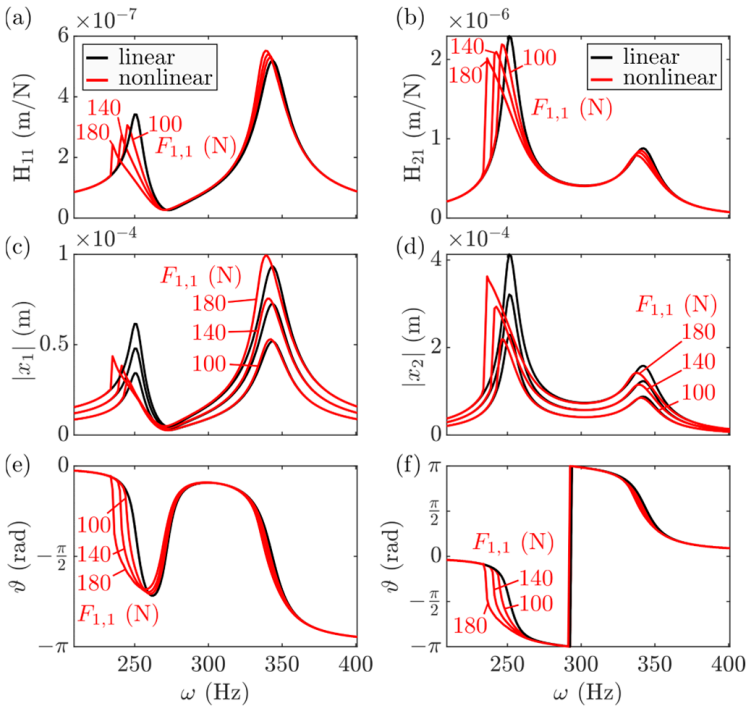


Figure 6. Comparison between the linear (black) and nonlinear (red) vibration absorbers with the mass ratio $\mu = 0.08$ kg/kg, for the given forcing amplitudes F_1. Although the two are significantly different from each other, both cases are effective within the bandwidth of interest. While panels (**a**) and (**b**) are the force normalized responses, panels (**c**,**d**) are the frequency responses, and panels (**e**,**f**) depict the corresponding phase lags.

In summary, we proposed a methodical approach to first identify the linear subsystems and then the underlying nonlinearity of the absorber. Then fine-tuning of the NTMD parameters is possible through numerical simulations. We emphasize that there is no

general solution to these problems. One has to set goals and constraints to achieve sufficient vibration attenuation with the introduced NTMD.

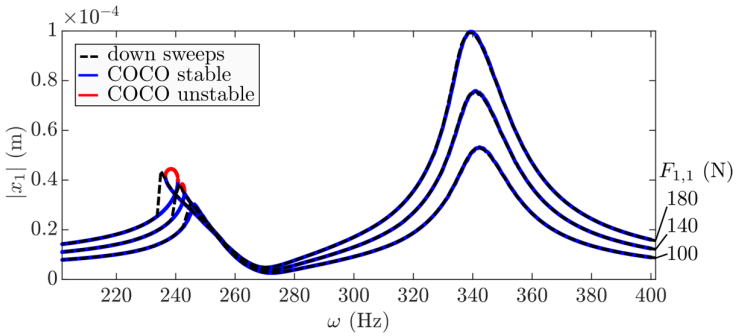


Figure 7. Comparing the frequency sweeps to numerical continuation (COCO). Although the sweeps are matching with the curves from the continuation software, we emphasize that complex behavior can occur [12], as the loops suggest, even for this simple example.

4. Conclusions

In this article, we demonstrate how to design a passive vibration absorber that attenuates the response amplitude of power electronic units at a given frequency band. First, the linear optimization is discussed. Then, the effective parameter selection of an NTMD is shown for the specific case with the PEUs.

A methodical approach is proposed, where one can set sufficient parameters for their NTMD design with given constraints in mind. First, the linear and nonlinear parameters have to be extracted for the accurate modeling of the observed coupled system. While the linear parameters can be addressed by small forcing amplitude measurement techniques related to the topic of experimental modal analysis, the nonlinear parameter extraction is rather challenging.

We used frequency sweeps with ensured constant forcing amplitudes to extract the phase resonance of the standalone absorber. After the system identification, a parameter analysis can be performed on the forcing amplitude and the mass ratio. By extracting the maximum response amplitudes of the attenuated system (within the frequency bandwidth of interest), an effective mass ratio can be found.

Author Contributions: Conceptualization, Á.S., B.D., S.S. and S.N.; methodology, Z.G.G., Z.G. and Z.D.; software, Z.G.G. and Z.G.; formal analysis, Z.G.G. and Z.G.; data curation, Á.S., B.D. and Z.G.; writing—original draft preparation, Z.G.G. and Z.G.; writing—review and editing, Z.G.G., Z.G., Z.D.; visualization, Z.G.G. and Z.G.; supervision, Z.D.; project administration, Z.G.G., Á.S., B.D., S.S. and S.N. All authors have read and agreed to the published version of the manuscript.

Funding: Project no. KDP-2023-C2254459 has been implemented with the support provided by the Ministry of Culture and Innovation of Hungary from the National Research, Development and Innovation Fund, financed under KDP-2023 funding scheme (Supported author: Z.G.G.).

Institutional Review Board Statement: Not applicable.

Informed Consent Statement: Not applicable.

Data Availability Statement: The data that support the findings of this study are available from Robert Bosch Kft., but restrictions apply to the availability of these data, which are not publicly available. Data are, however, available from the authors upon reasonable request and with permission of Robert Bosch Kft.

Conflicts of Interest: Authors Zoltan Gabor Gazdagh, Ádám Szabó, Bálint Dobrovics, Szargisz Szargszjan, Szabolcs Nagy were employed by the company Robert Bosch Kft. The remaining authors declare that the research was conducted in the absence of any commercial or financial relationships

that could be construed as a potential conflict of interest. The authors declare that this study received funding from the National Research, Development and Innovation Fund of Hungary (KDP-2023; Project No. KDP-2023-C2254459). The funder was not involved in the study design, data collection, analysis, or interpretation, the writing of this article, or the decision to submit it for publication. Author Z.G.G. received this funding; all other authors declare no competing interests.

References

1. Li, X.; He, L.; Hu, M.; Ye, W. Study of integrated system on power electronics unit for electric vehicle. In *IOP Conference Series: Materials Science and Engineering, Proceedings of 2018 3rd International Conference on Insulating Materials, Material Application and Electrical Engineering, Melbourne, Australia, 15–16 September 2018*; IOP Publishing: Bristol, UK, 2018; Volume 452, p. 032083.
2. Szabó, V.; Vehovszky, B.; Gazdagh, Z.G. Dynamic and quasi-static stiffness characterization of a lamination stack of an electric motor. *Heliyon* **2024**, *10*, e39693. [CrossRef] [PubMed]
3. Den Hartog, J.P. *Mechanical Vibrations*; Dover Publications Inc.: New York, NY, USA, 1985; pp. 87–102.
4. Sims, N.D. Vibration absorbers for chatter suppression: A new analytical tuning methodology. *CIRP Ann.* **2007**, *56*, 335–338. [CrossRef]
5. Dekemele, K.; Van Torre, P.; Loccufier, M. Design, construction and experimental performance of a nonlinear energy sink in mitigating multi-modal vibrations. *J. Sound Vib.* **2020**, *473*, 115243. [CrossRef]
6. Ewins, D.J. *Modal Testing: Theory, Practice and Application*, 2nd ed.; John Wiley & Sons: Chichester, UK, 2009.
7. Kerschen, G.; Worden, K.; Vakakis, A.F.; Golinval, J.C. Past, present and future of nonlinear system identification in structural dynamics. *Mech. Syst. Signal Process.* **2006**, *20*, 505–592. [CrossRef]
8. Gabos, Z.; Dombovari, Z. Open-loop swept frequency response of nonlinear structures subjected to weak coupling. *Nonlinear Dyn.* **2025**, *113*, 5091–5108. [CrossRef]
9. Nayfeh, A.H.; Mook, D.T. *Nonlinear Oscillations*; John Wiley & Sons: Hoboken, NJ, USA, 2024.
10. Volvert, M.; Kerschen, G. Resonant phase lags of a Duffing oscillator. *Int. J. Non-Linear Mech.* **2022**, *146*, 104150. [CrossRef]
11. Dankowicz, H.; Schilder, F. (Eds.) *Recipes for Continuation*; Society for Industrial and Applied Mathematics: Philadelphia, PA, USA, 2013.
12. Dekemele, K.; Habib, G. Softening versus hardening nonlinear energy sinks: Forced vibration control and isolated resonance curves. *Nonlinear Dyn.* **2025**, *113*, 19179–19198. [CrossRef]

Disclaimer/Publisher's Note: The statements, opinions and data contained in all publications are solely those of the individual author(s) and contributor(s) and not of MDPI and/or the editor(s). MDPI and/or the editor(s) disclaim responsibility for any injury to people or property resulting from any ideas, methods, instructions or products referred to in the content.